Proceedings of ERAD (2002): 277–281 © Copernicus GmbH 2002

ERAD 2002

Evaluation of polarimetric radar rainfall algorithms at X-band

V. Chandrasekar[1], **E. Gorgucci**[2], **and L. Baldini**[2]

[1]Colorado State University, Fort Collins CO 80523, Colorado, USA
[2]Istituto di Scienze dell'Atmosfera e del Clima (CNR) Area di Ricerca Roma-Tor Vergata, Via del Fosso del Cavaliere, 100-00133 Rome, Itlay

Abstract. Electromagnetic waves are attenuated significantly due to precipitation at X-band, and the attenuation is determined by the intensity of precipitation. Since the introduction of the polarimetric radar, some fairly successful attenuation correction algorithms have been developed. In addition measurements based on differential phase are not affected by attenuation. This paper presents evaluation of dual-polarization radar rainfall algorithms at X-band. The analysis shows the intuitive result that specific differential propagation phase based estimates can be used at much lower rainfall rates in comparison to S-band.

1 Introduction

The most commonly used polarimetric radar measurements in rainfall estimation are the reflectivity factor, usually at horizontal polarization (Z_h), differential reflectivity (Z_{dr}) and specific differential propagation phase (K_{dp}). Based on the above three measurements, a number of algorithms have been derived in the literature to estimate rainfall (see Bringi and Chandrasekar, 2001 for a summary of references). These algorithms have been derived assuming equilibrium raindrop shapes, described by a specific shape-size relationship (Pruppacher and Beard, 1970). The mean axis ratio versus size relation is crucial for deriving algorithms that use Z_{dr} and K_{dp}. Chandrasekar et al. (1990) indicated based on K_{dp} analysis at S-band that at low rainfall rates, the radar rainfall algorithms have large measurement error. However K_{dp} directly scales with frequency, and has a higher dynamic range at X-band. This feature makes K_{dp} at X-band more useful at low rainrates. Along with the advantages, X-band measurements come with their own problems, the significant ones being, attenuation, differential attenuation and phase shift on backscatter (Matrosov et al., 1999). A recent study by Keenan et al. (1997) indicates that K_{dp}-based polarimetric radar rainfall algorithms are influenced by deviation from the equilibrium shape of raindrops. Gorgucci et al. (2000) demonstrated that the slope of a linear mean raindrop shape-size relation can be estimated from polarimetric radar measurements which can be used subsequently in rainfall rate estimation parameters. This paper presents comparison of algorithms to estimate rainfall rate using polarimetric radar measurements at S- (2.8 GHz) and X- (9.3GHz) band.

Correspondence to: E. Gorgucci
(gorgucci@radar.ifa.rm.cnr.it)

2 Polarimetric radar measurements and rainfall algorithms

The distribution of raindrop sizes and shapes determines the electromagnetic scattering properties of rain-filled media. These effects, in turn, are embodied in radar measurements such as, reflectivity factors ($Z_{h,v}$) at h and v polarization states, differential reflectivity (Z_{dr}), which is the ratio of reflectivities at the two polarization states, and specific differential phase (K_{dp}) which is due to the propagation phase difference between the two polarizations. The raindrop size distribution (RSD) can be expressed as (Chandrasekar and Bringi, 1987)

$$N(D) = n_c f(D) \quad (\mathrm{mm}^{-1}\ \mathrm{m}^{-3}) \tag{1}$$

where $N(D)$ is the number of the raindrops per unit volume per unit size interval (D to $D + \Delta D$), n_c is the concentration and $f(D)$ is a probability density function. Theoretical, experimental studies as well as polarimetric radar measurements show that the raindrop shapes can be approximated by an oblate spheroid with the axis ratio (b/a) given as,

$$r = \frac{b}{a} \approx 1.03 - \beta D \tag{2}$$

where D is the equivolumetric spherical diameter (typically in units of mm), a and b are the major and minor axes of the spheroid. A commonly used value for β is 0.062, which is a linear fit to the wind-tunnel data of Pruppacher and Beard (1970). The radar observables namely, $Z_{h,v}$, Z_{dr}, and K_{dp} can be expressed in terms of the RSD as follows:

$$Z_{h,v} = \frac{\lambda^4}{\pi^5 |k|^2} \int \sigma_{h,v}(D) N(D) dD \quad (\mathrm{mm}^6\ \mathrm{m}^{-3}) \tag{3}$$

where $\sigma_{h,v}$ represent the radar cross sections at horizontal and vertical polarizations, respectively; λ the wavelength, and $k=(\varepsilon r-1)/(\varepsilon_r+2)$ where ε_r is the dielectric constant of water;

$$Z_{dr}=10\log_{10}(Z_h/Z_v) \tag{4}$$

$$K_{dp}=\frac{108\lambda}{\pi}\Re\int\Big[f_h(D)-f_v(D)\Big]N(D)dD\ (\text{deg km}^{-1}) \tag{5}$$

where $\Re$ refers to real part of a complex number and f_h and f_v are the forward-scatter amplitudes at h and v polarization, respectively.

Radar measurements used in polarization diversity radar estimates of rainfall rate are, Z_h (mm^6 m^{-3}), Z_{dr} (dB) and K_{dp} (deg km^{-1}). A number of algorithms have been introduced in the literature for estimation of rainfall using radar measurements from a polarization diversity radar operating in the linear polarization basis. In this paper we focus on algorithms that have been used extensively in the literature. These algorithms can be broadly classified into three categories, namely: (a) algorithms that use reflectivity and differential reflectivity, $R(Z_h, Z_{dr})$, (b) algorithms that use differential propagation phase, $R(K_{dp})$, and (c) algorithms that use differential propagation phase and differential reflectivity, $R(K_{dp}, Z_{dr})$. These algorithms have the form,

$$R(Z_h,Z_{dr})=c_1Z_h^a10^{b_1Z_{dr}} \tag{6}$$

$$R(K_{dp})=c_2K_{dp}^{a_2} \tag{7}$$

$$R(K_{dp},Z_{dr})=c_3K_{dp}^{a_3}10^{-0.1b_3Z_{dr}} \tag{8}$$

3 Scaling of measurements with frequency

Under Rayleigh scattering assumptions reflectivity factor given by Eq. (3) can be approximated as

$$Z=\int D^6N(D)dD \tag{9}$$

Under Rayleigh scattering approximation, the reflectivity will not change with frequency. However at X-band frequencies, Rayleigh scattering assumptions are not completely valid, and as a result the reflectivity will change. Figure 1 shows a scatter plot of reflectivity at X- and S-bands. It can be seen from Fig. 1 that above 30 dBz, there is a difference in reflectivity that keeps increasing with reflectivity. Similarly Z_{dr} values differ due to non-Rayleigh scattering for values above 1 dB. K_{dp} scales directly with frequency (valid upto 13 GHz). Observing the variability in the dynamic range of measurements, the error structure of rainfall algorithms that use Z_h and Z_{dr} are likely to remain similar between S- and X-bands. However algorithms that use K_{dp} are likely to be very different. Because of the increased K_{dp} values at X-band (for the same rainrate) it is expected that $R(K_{dp})$ could be used at smaller rainrates. If the prevailing β is known fairly well, then it is certain that $R(K_{dp})$ will be useful at smaller rainrates. Attenuation induced effects will affect Z_h and Z_{dr}, but not K_{dp}. However K_{dp} will be contaminated by the phase shift on backscatter δ, which can be of the order of 8–12 degrees at X-band. This needs to be dealt with at regions of radial gradients, where a radial change of δ could be interpreted as differential propagation phase.

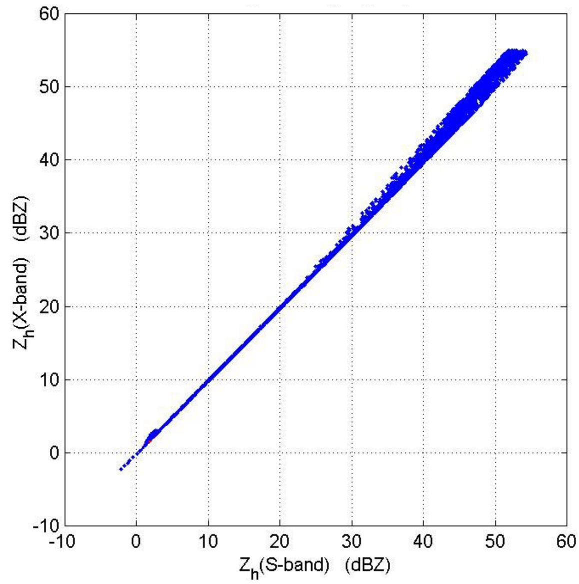

Fig. 1. Scatterplot between reflectivity at S-band versus the corresponding value at X-band for widely varying RSD.

4 Rainfall algorithms

Gorgucci et al. (2000) have shown that an estimate of β can be obtained from Z_h, Z_{dr} and K_{dp}. Similar parameterization can be obtained at X-band as

$$\hat{\beta}_x=0.589Z_v^{-0.292}10^{0.1142Z_{dr}}K_{dp}^{0.292} \tag{10}$$

Equation (10) estimates β to an accuracy of 5% with negligible bias. Estimating the prevailing 'β' is important in developing rainfall algorithms.

4.1 $R(Z, Z_{dr})$ algorithm

The generic form of the $R(Z, Z_{dr})$ algorithm can be written as

$$R=a_1Z_h^{b_1}\ \xi_{dr}^{c_1} \tag{11}$$

where $Z_{dr}=10\log_{10}(\xi_{dr})$. The expressions for a, b, c at S-band were provided by Gorgucci et al. (2001). The corresponding algorithm for X-band is given by $a_1=0.623\beta^{1.44}$, $b_1=0.964$, $c_1=-1.02\beta^{-0.056}$.

Figure 2 shows a scatter plot of R obtained from Eq. (11) as a function of true rainfall rate. The result of Fig. 1 indicates that this parameterization yields rainfall estimates fairly accurately with a normalized standard deviation of 13.5%, and a correlation coefficient of 99.6%. It should be noted that these do not have measurement errors or attenuation correction in them.

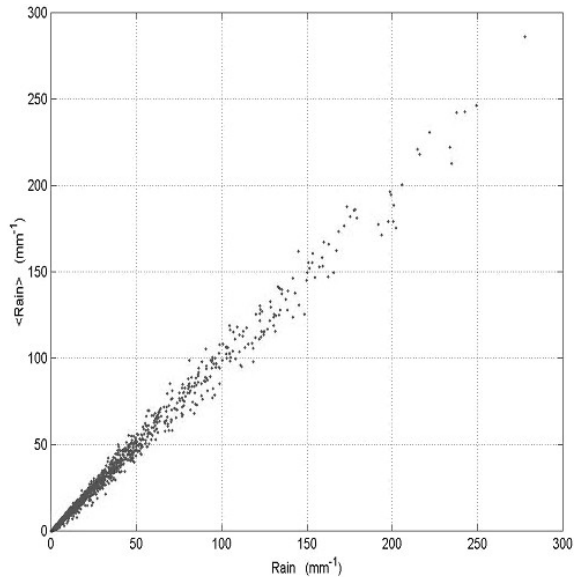

Fig. 2. Scatterplot of $R(Z_h, Z_{dr})$ versus the true rain value at X-band.

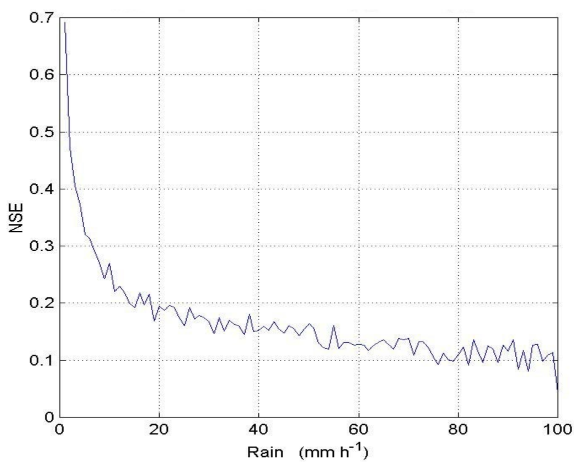

Fig. 3. Normalized standard error of $R(K_{dp})$ parameterisation.

4.2 $R(K_{dp})$ algorithm

The parameterization of $R(K_{dp})$ at X-band is given by

$$R(K_{dp}) = a_2 K_{dp} \tag{12}$$

where $a_2 = 0.278\beta^{-1.33}$.

The parameterization shown in Eq. (12) is nearly unbiased similar to that of Eq. (11), however has a higher standard deviation. Figure 3 presents the normalized standard error of $R(K_{dp})$ given by Eq. (12), as a function of rainfall rate. It can be seen from Fig. 3 that the parameterization is fairly accurate with an error of about 20% at 20 mm/hr and 15% at 40 mm/hr.

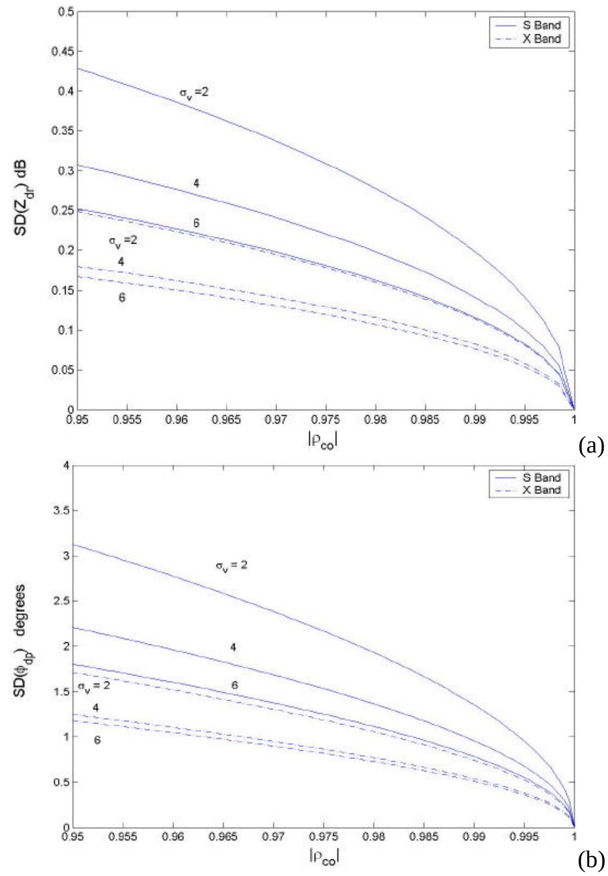

Fig. 4. Error structure of Z_{dr} and K_{dp} at S- and X-band (hybrid mode with 128 samples) shown as a function of ρ_{co} for various values of Doppler spectral widths (σ_v) (a) shows the standard deviation of Z_{dr} and (b) shows the standard deviation of ϕ_{dp}.

4.3 $R(K_{dp}, Z_{dr})$

The best parameterization for $R(K_{dp},\ Z_{dr})$ at X-band is given by

$$R = a_3 K_{dp}^{b_3}\, \zeta_{dr}^{c_3} \tag{13}$$

where $a_3 = 0.0734\beta^{-1.99}$, $b_3 = 1.27\beta^{0.0935}$, $c_3 = -4.71 \times 10^{-3}\beta^{-1.92}$.

The above estimator estimates rainfall rate to an accuracy of 13%. Again it should be noted that these estimates are obtained without considering measurement error and attenuation.

5 Measurement errors, impact of attenuation and phase shift on backscatter

5.1 Measurement error

The measurement error of Z_h at S- and X-bands are likely to be of the similar order. For a statistically stationary radar signal, measurement of Z_h at X-band should be more accurate

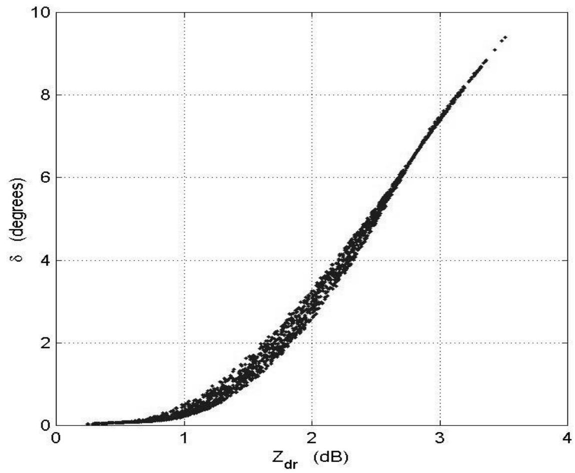

Fig. 5. Scatterplot of δ versus differential reflectivity, Z_{dr}.

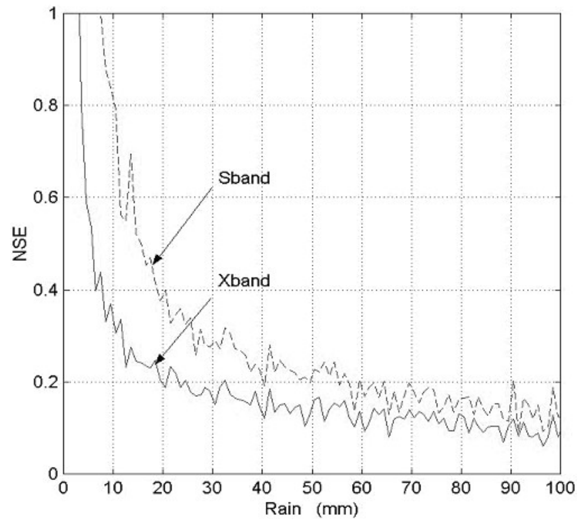

Fig. 6. Normalized Standard Error in the estimate of the rainrate for X- and S-band as a function of the rainrate for a 7.5 Km path.

than that at S-band. The accuracy of Z_{dr} and ϕ_{dp} depends on the mode of operation. The accuracies could be widely different between hybrid mode and alternating mode of operation (see Bringi and Chandrasekar, 2001 for details). For simplicity only hybrid mode of operation is considered here. Figure 4a shows the standard deviation of Z_{dr} as a function of the copolar correlation coefficient (ρ_{co}), where as Fig. 4b shows the standard deviation of ϕ_{dp} as a function of ρ_{co}. It can be seen from Fig. 4 that Z_{dr} and ϕ_{dp} can be estimated to an accuracy of similar orders in both S- and X-bands.

5.2 Attenuation correction

Attenuation correction is important at X-band and due to the extent of attenuation. The extent of attenuation can be easily estimated from the amount of cumulative ϕ_{dp} in rain. Using a simple linear approximation between the specific attenuation, differential attenuation and K_{dp}, a simple estimate of attenuation and differential attenuation can be obtained as

$$A = \alpha_A \phi_{dp} \tag{14}$$

and

$$A_{DP} = \alpha_{dp} \phi_{dp} \tag{15}$$

where α_A and α_{dp} take values of 0.2 and 0.035 approximately (depending on the raindrop shape model). There are more detailed procedures available for attenuation correction (see Bringi and Chandrasekar, 2001 for a summary and the references contained therein). This is a detailed topic and the discussion is limited for brevity.

5.3 Phase shift on backscatter (δ)

Unlike lower frequencies phase shift on backscatter is larger at X-band in rain. The best parameter to correlate it with is Z_{dr}. Figure 5 shows a plot of δ versus Z_{dr} at X-band, and the results indicate that δ can be as much as 10 degrees. This must be considered in the estimate of K_{dp}, specially in regions of large gradients in rainfall rate of Z_{dr}.

6 Comparison of algorithms

Attenuation correction is important in using algorithms that involve Z_h and Z_{dr} and the procedure is fairly detailed and is skipped here for brevity. A comparison of $R(K_{dp})$ between S- and X-band is presented. Figure 6 shows a comparison of the normalized standard error in $R(K_{dp})$ between S- and X-band including the effect of measurement algorithms. This evaluation assumes a simple model that the prevailing 'β' (raindrop shape) is known and need not be estimated. Therefore this presents the best scenario. The evaluation assumes a path length of 7.5 km and β is fixed at 0.062. Figure 6 shows the NSE of $R(K_{dp})$ at X-band and S-band simultaneously. It can be seen that $R(K_{dp})$ at X-band performs better than S-band results. Specifically Chandrasekar et al. (1990) concluded that $R(K_{dp})$ is the best estimate at S-band above 60–70 mm h^{-1}. It appears that similar accuracy can be obtained from 20 mm h^{-1} onwards at X-band.

7 Summary

This paper presents an evaluation of X-band algorithms for rainfall estimate. This topic is fairly extensive and only limited results are presented. The results estimate the exact rain rates at which X-band can be used to achieve accuracies similar to S-band. The analysis confirms the intuitive result that X-band rainfall estimates using $R(K_{dp})$ can be used starting about one third the rain rate at which S-band algorithms are accurate. Attenuation correction related issues have been evaluated but not presented for brevity.

Acknowledgement. This research is supported by the NASA TRMM program, the National Group for Defense from Hydrological Hazard (CNR, Italy) and by the Italian Space Agency (ASI).

References

Bringi, V.N. and V. Chandrasekar, Polarimetric Doppler Weather Radar: Principles and applications, Cambridge Univ. Press, 2001

Chandrasekar, V., V.N. Bringi, N. Balakrishnan, and D.S. Zrnic, "Error structure of multiparameter radar and surface measurements of rainfall. Part III: Spexific differential phase," J. Atmos. Oceanic Technol., vol. 7, pp. 621-629, 1990

Chandrasekar, V. and V.N.Bringi, "Simulation of Radar Reflectivity and Surface Measurements of Rainfall," J. Atmos. Ocean.tech., vol. 4, pp. 464-478, 1987

Gorgucci, E., G. Scarchilli, V. Chandrasekar, and V. N. Bringi, "Measurement of mean raindrop shape from polarimetric radar observation," J. Atmos. Sci., vol. 57, pp. 3406-3413, 2000

Gorgucci, E., G. Scarchilli, V. Chandrasekar, V.N. Bringi, "Rainfall Estimation from Polarimetric Radar Measurements: Composite Algorithms Immune to Variability in Raindrop ShapeSize Relation," Journal of Atmospheric and Oceanic Technology, vol. 18, pp. 1773-1786, 2001

Keenan, T.D., P. T. May, D. S. Zrnic, L. D. Carey, and S. A. Rutledge, "Sensitivity of C-band polarimetric variables to propagation and backscatter effects in rain," Preprints, 28th Conf. on Radar Meteorology, Austin, Texas, Amer. Meteor. Soc., pp. 13-14, 1997

Pruppacher, H.R. and K.V. Beard, "A wind tunnel investigation of the internal circulation and shape of water drops falling at terminal velocity in air," Quart. J. Roy. Meteor. Soc., vol. 96, pp. 247-256, 1970

Matrosov, Sergey Y., Robert A. Kropfli, Roger F. Reinking, Brooks E. Martner, 1999: Prospects for Measuring Rainfall Using Propagation Differential Phase in X- and Ka-Radar Bands. Journal of Applied Meteorology: Vol. 38, No. 6, pp. 766776.